




Biflavonoids from *Rhus succedanea* as probable natural inhibitors against SARS-CoV-2: a molecular docking and molecular dynamics approach

Kiran Lokhande^a, Neelu Nawani^b, Swamy K. Venkateswara^c and Sarika Pawar^b 

^aDr. D. Y. Patil Vidyapeeth, Bioinformatics Research Laboratory, Dr. D. Y. Patil Biotechnology and Bioinformatics Institute, Pune, India;

^bDr. D. Y. Patil Vidyapeeth, Microbial Diversity Research Centre, Dr. D. Y. Patil Biotechnology and Bioinformatics Institute, Pune, India;

^cBioinformatics Research Group, MIT School of Bioengineering Sciences & Research, MIT-ADT University, Pune, Maharashtra, India

Communicated by Ramaswamy H. Sarma

ABSTRACT

The recent outbreak of SARS-CoV-2 has quickly become a worldwide pandemic and generated panic threats for both the human population and the global economy. The unavailability of effective vaccines or drugs has enforced researchers to hunt for a potential drug to combat this virus. Plant-derived phytochemicals are of applicable interest in the search for novel drugs. Bioflavonoids from *Rhus succedanea* are already reported to exert antiviral activity against RNA viruses. SARS-CoV-2 Mpro protease plays a vital role in viral replication and therefore can be considered as a promising target for drug development. A computational approach has been employed to search for promising potent bioflavonoids from *Rhus succedanea* against SARS-CoV-2 Mpro protease. Binding affinities and binding modes between the biflavonoids and Mpro enzyme suggest that all six biflavonoids exhibit possible interaction with the Mpro catalytic site (−19.47 to −27.04 kcal/mol). However, Amentoflavone (−27.04 kcal/mol) and Agathisflavone (−25.87 kcal/mol) interact strongly with the catalytic residues. Molecular dynamic simulations (100 ns) further revealed that these two biflavonoids complexes with the Mpro enzyme are highly stable and are of less conformational fluctuations. Also, the hydrophobic and hydrophilic surface mapping on the Mpro structure as well as biflavonoids were utilized for the further lead optimization process. Altogether, our findings showed that these natural biflavonoids can be utilized as promising SARS-CoV-2 Mpro inhibitors and thus, the computational approach provides an initial footstep towards experimental studies in *in vitro* and *in vivo*, which is necessary for the therapeutic development of novel and safe drugs to control SARS-CoV-2.

RESEARCH HIGHLIGHTS

1. *Rhus succedanea* biflavonoids have antiviral activity.
2. The molecular interactions and molecular dynamics displayed that all six biflavonoids bound with a good affinity to the same catalytic site of Mpro.
3. The compound Amentoflavone has a strong binding affinity (−27.0441 kcal/mol) towards Mpro.
4. The binding site properties of SARS-CoV-2-Mpro can be utilized in a novel discovery and lead optimization of the SARS-CoV-2-Mpro inhibitor.

ARTICLE HISTORY

Received 30 July 2020

Accepted 22 November 2020

KEYWORDS

Coronavirus; SARS-CoV-2; COVID-19; Mpro protein; *Rhus succedanea*; biflavonoids; molecular docking; molecular dynamics simulation


1. Introduction

At the end of December 2019 a sudden outbreak of SARS-CoV-2, a new class of coronavirus, which causes Corona Virus Disease in the year 2020 (COVID-19), had initially appeared in Wuhan, China and very soon spread worldwide generating a pandemic condition. Nearly 47,362,304 infected people and around 12,11,986 (till 05 November 2020) deaths by this virus posed a serious civic health problem, as reported by WHO (World Health Organization, 2020) and continue to do so at an alarming rate. The major strategies employed by different countries to treat SARS-CoV-2 are personal care by a physical intervention such as self-quarantine services and physical/social distancing, administration of anti-

malarial and anti-HIV drugs (Etaware, 2020; WHO, 2020). To date, no specific and potent drugs have been manufactured against SARS-CoV-2. Therefore, there is an urgent need to develop and design potent drug and/or vaccine candidates against this pandemic causing virus (Kumar et al., 2020; Pandeya et al., 2020).

The SARS-CoV-2 viral genome encodes around 20 proteins, amongst which chymotrypsin-like cysteine proteinase (3CLpro or Mpro) is vital for virus replication. The activity of Mpro is thought to be regulated by cleavage site-specificity. This protease has 11 putative cleavage positions indicating its prevalence in proteolytic processing (Yang et al., 2003; Zhang et al., 2020). The Mpro has been found as a potential target to design and developing drugs against SARS-CoV-2

CONTACT Sarika Pawar  sarika.pawar@dpu.edu.in; saavipawar@gmail.com  Dr. D. Y. Patil Vidyapeeth, Microbial Diversity Research Centre, Dr. D. Y. Patil Biotechnology and Bioinformatics Institute, Pune, India.

 Supplemental data for this article can be accessed online at <https://doi.org/10.1080/07391102.2020.1858165>

(Amin et al., 2020; Amin & Jha, 2020; Enmozhi et al., 2020; Ghosh et al., 2020; Goyal & Goyal, 2020; Li & Kang, 2020; Ullrich & Nitsche, 2020;) since very little similarity with human proteases makes the drugs less toxic to humans (Anand et al., 2002; Joshi et al., 2020). Therefore, finding promising natural inhibitors for the Mpro can hinder the SARS-CoV-2 virus replication in the host cell and reduce its infectivity (Havranek & Islam, 2020; Dong & Gao, 2020).

Since ancient times in traditional medicine, plants derived flavonoids have been utilized as a source of non-toxic and safe bioactive compounds, to treat several viral infections (Cazarolli et al., 2008; Harborne & Williams, 2000). Recently, several studies have revealed that many bioactive compounds from different medicinal plants act as promising inhibitors against coronavirus (in review, Siddiqui et al., 2020a, 2020b). Recently, Surti and coworkers have discovered that Ilimaquinone (marine sponge metabolite) as a novel inhibitor of SARS-CoV-2 key target proteins in comparison with suggested COVID-19 drugs (hydroxychloroquine, azithromycin, favipiravir, ivermectin and remdesivir) (Surti et al., 2020). In addition, many antiviral phytochemicals from green tea (catechins or polyphenols); from Indian spices (Rosmanol, Carnosol and Arjunglucoside-I); from buriti oil (*Mauritia flexuosa* L.) are proposed to be promising against SARS-CoV-2 Mpro protease (Costa et al., 2020; Das et al., 2020; Ghosh et al., 2020; Umesh et al., 2020)

R. succedanea (formerly *Toxicodendron succedaneum*) also known as 'japanese tallow or wax tree' belonging to the *Anacardiaceae* family is one of the plants with many medicinal properties. This plant is widely distributed in Asia and used as an Ayurvedic remedy for quite a long time to treat common cold, cough, asthma, diarrhea and dysentery. In addition, it has antioxidant activity and the potential to suppress gastritis (Khan et al., 2016; Kim et al., 2018; Shrestha et al., 2013; Wu et al., 2002). To date, several bioactive phytochemicals such as tannins, biflavonoids, and phenols from different parts of *R. succedanea* have been extracted, characterized and analyzed for anti-viral activity (Chen & Lin, 1975, 1976; Fa-Ching et al., 1974; Khan et al., 2020). Information on the molecular structure of biflavonoids offers a chance to explore and identify promising pharmacological activity against SARS-CoV-2 (Sharma et al., 2020).

In this context, the projection and development of novel non-toxic drugs have marched in the last two decades, from the use of innovative complementary techniques such as computational tools (Meng et al., 2011). Molecular docking and molecular dynamics simulation are two major computational methods that provide great applicability in pharmaceutical research industries in search of novel drugs in a short duration time and assist experimental studies (Alonso et al., 2006). The molecular docking technique assists to predict the best fit of the screen ligand in the catalytic cavity of a targeted protein which has been previously reported (Wang & Zhu, 2016). While as, molecular dynamics simulation analyzes the distribution and physical movements of the atoms and molecules for a fixed period which provides a view of the dynamic evolution of the protein-ligand system (De Vivo et al., 2016).

The several medicinal applications of *Rhus succedanea* are well reported. However, in the current pandemic situation of SARS-CoV-2, its anti-viral properties are greatly significant. All together due to its anti-viral, anti-oxidant and immunomodulatory potentials, this plant's biflavonoids could become a promising therapeutic alternative against Covid-19. The present work carried out preliminary *in silico* analysis with the application of molecular docking and molecular dynamics of the biflavonoids from *R. succedanea* against SARS-CoV-2 Mpro, in order to find out promising enzyme inhibitors against the Mpro protease to control Covid-19.

2. Materials and methods

2.1. The *in silico* preparation of Mpro crystal structure and its sequence analysis

The three-dimensional (3D) X-ray crystalized structure of SARS-CoV-2 Mpro which is complexed with N3 inhibitor (PDB ID: 6LU7) (Jin et al., 2020) was downloaded from the RCSB Protein Data Bank (<https://www.rcsb.org/>). The structure of Mpro contains two chains (Chain A and Chain B) which are homodimeric forms. In this study, we have selected Chain A of Mpro and prepared the structure using Schrodinger's Protein Preparation Wizard (PPW) and used it for the molecular docking calculations.

To reveal the conserved residues of the functional domain that are related to the molecular function of the SARS-CoV-2 Mpro structure, the NCBI CD (Conserved Domain) database (<https://www.ncbi.nlm.nih.gov/Structure/cdd/wrpsb.cgi>) was used. The binding site residues are considered which are present within the vicinity of 6.5 Å from co-crystal ligand, i.e. N. 3. The binding site residues, Thr24, His41, Cys44, Phe140, Thr26, Gly143, His164, Leu27, Glu166, His172, Leu141, Thr190, Asn142, Gln189, and Gln192 have occupied the binding cavity of Mpro.

2.2. Retrieval of biflavonoid compounds of *R. succedanea*

The two-dimensional (2D) structures of biflavonoids from like Amentoflavone (CID 5281600), Agathisflavone (CID 5281599), Robustaflavone (CID 5281694), Hinokiflavone (CID 5281627), Rhusflavanone (CID 466314), and Succedaneaflavanone (CID 12114301) were downloaded from the PubChem (<https://pubchem.ncbi.nlm.nih.gov/>) (Figure 1). These retrieved six flavonoids compounds were subjected to energy minimization using the Maestro software (Schrodinger Release 2019-4) with an OPLS-2005 force field, the process of energy minimization continued till an energetically (thermodynamically) stable confirmation is achieved. These stable and processed conformers of flavonoids compounds were subjected to molecular docking calculations with COVID-19 Mpro.

2.3. Molecular docking calculations

Intermolecular interaction between *R. succedanea* biflavonoids and Mpro, molecular docking simulation, was achieved

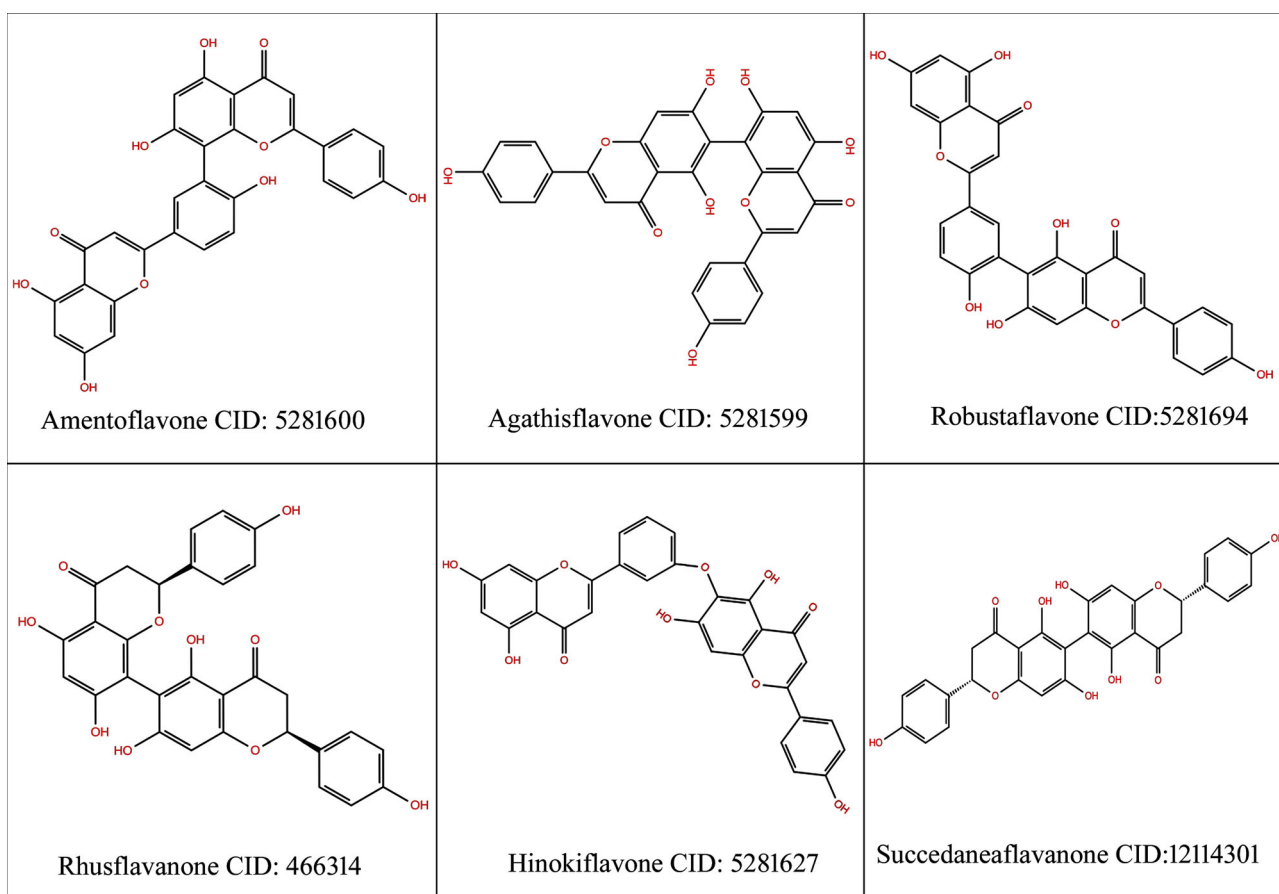


Figure 1. The 2D chemical structure of biflavonoids with their PubChem CID from *R. succedanea* plant.

by using commercial FlexX software (LeadIT version 2.3.2; BioSolveIT, 2017). The prepared structure of Mpro is kept as a rigid structure throughout the docking simulations. The binding pocket of the Mpro was well-defined using the receptor preparation panel of FlexX considering above mentioned binding site residues. The prepared biflavonoids compounds are then subjected to molecular docking calculations, to evaluate the binding pose/conformations and binding affinity in the binding cavity of Mpro. The docking calculations were calculated with FlexX software by implementing systematic ligand conformational expansion followed by its placement in the binding cavity of the Mpro.

The docking energy of FlexX not only depends on H-bond interaction but also on the scoring function, short-ranged electrostatic interactions and van der Waals interactions, the solvation energy and loss of entropy after ligand binding. The best conformations of a flavonoid compound with good binding affinity with Mpro are evaluated by binding energy and intermolecular interaction.

2.4. Molecular dynamic (MD) simulation

To assess the binding intensity/strength and stability of reported biflavonoids with SARS CoV-2 Mpro, 100 ns time scale molecular dynamic simulations were performed using Desmond software (Schrödinger Release 2019-4: Desmond) which is a highly integrated tool that set up the biological and chemical system simulations integrated with a molecular

modeling environment. The MD simulation computes the dynamic behavior of the receptor upon binding of macromolecule or ligand. Desmond's system builder utility available in the Maestro program was used for the solvation and ionization of the SARS-CoV-2 receptor complexed with lead compounds. The explicit solvent i.e. three-point (TIP3) water model was immersed to solvate the SARS CoV-2 Mpro-biflavonoids complex system in the cubic box of 10 Å buffer size having a periodic boundary condition to approximate the infinite system (Lokhande et al., 2019). The total number of water molecules and the used counter ions to neutralize the complex are reported in Table 1.

The steepest descent method was used to minimize the complex system energetically with the OPLS-2005 force field. The 100 ns time scale MD simulations for each complex were performed at constant NPT (N=Number of Atoms, P=Pressure, and T=Temperature) ensemble. Throughout the equilibrations, systems were coupled with the Martyna-Tobias-Klein barostat method for controlling pressure at 1 atm and the temperature was regulated by using velocity rescaling Nose Hoover chain thermostat method at 300 K. The M-SHAKE algorithm was used to constrain the bond length of hydrogen atoms. Cut off for short-range electrostatics and Van Der Waals interactions are maintained at 1 nm. Also, the long-range Coulomb electrostatic interactions were calibrated through particle mesh Ewald (PME) summation. The leap-frog algorithm was used to compute the equation of motion with a time step of 2 fs (Lokhande et al.,

Table 1. Details of Molecular dynamics simulation.

Biflavonoid with SARS-CoV-2 Mpro	Immersed water molecules (TIP3P)	Total charge of the complex	Counter ion	Counter ion concentration
Amentoflavone	17,995	−4	4 Na ⁺	4.042 μM
Agathisflavone	17,995	−4	4 Na ⁺	4.042 μM
Robustaflavone	17,990	−4	4 Na ⁺	4.042 μM
Rhusflavanone	17,991	−4	4 Na ⁺	4.042 μM
Hinokiflavone	17,992	−4	4 Na ⁺	4.042 μM
Succedaneafavanone	17,991	−4	4 Na ⁺	4.042 μM

2020a). The conformational changes in the SARS-CoV-2 Mpro C- α backbone atoms of the after binding of biflavonoids were compared with the initial conformations of a crystal structure (PDB ID: 6LU7) in terms of Root Mean Square Deviation (RMSD). Also, the fluctuations in the amino acids of SARS-CoV-2 Mpro after binding of the lead compounds were computed using the trajectories generated during the 100 ns MD simulation and presented as Root Mean Square Fluctuation (RMSF) graph.

2.5. Binding free energy calculations

The Prime (Jacobson et al., 2004) module of the Schrodinger software was used to compute the binding free energies for the complexes of SARS-CoV-2 Mpro and lead compounds in terms of Molecular Mechanics, the Generalized Born Model and Solvent Accessibility (MM/GBSA). The various compiled van der Waals interactions and the nonpolar solvent accessible surface area along with advanced OPLS-2005 force field, polar solvation (GSGB), Molecular Mechanics Energies (EMM), and non-polar solvation (GNP) were used in the Prime to calculate binding free energies of bound complexes. The following equation was employed to compute the binding free energies changes during the 100 ns MD simulation of SARS-CoV-2 Mpro complexes with reported lead compounds.

$$\Delta G_{\text{bind}} = G_{\text{complex}} - (G_{\text{protein}} + G_{\text{ligand}}),$$

$$G = \text{GSGB} + \text{EMM} + \text{GNP}$$

where G_{complex} is the Protein-Ligand complex energy, G_{protein} is the Protein-energy, G_{ligand} is the unbound ligand energy. Also, the EMM, SGB and GSGB represent molecular mechanics energies, nonpolar solvation model and polar solvation model respectively.

2.6. Hydrophobic and hydrophilic surface maps for SARS-CoV-2-Mpro structure

Hydrophobic/philic Surfaces panel of Maestro was used to generate hydrophobic and hydrophilic Surface maps on the SARS-CoV-2-Mpro structure as well as biflavonoids compound. The Hydrophobic/philic map is calculated to help in visualizing favored locations and properties of ligand atoms in receptor active site. Given a Mpro structure, the accessible space by the ligand in the active site is partitioned into hydrophobic and hydrophilic regions. In this report, hydrophobic and hydrophilic map assist to reveal favorable hydrophobic and hydrophilic ligand groups in the binding pocket of SARS-CoV-2-Mpro. Also, we have reports, the hydrophobic and hydrophilic surface area of ligand atoms in the SARS-

CoV-2-Mpro cavity, which can aid in the design and development of new ligands.

3. Results and discussion

3.1. The SARS-CoV-2-Mpro catalytic domain

The NCBI CD search results revealed the catalytic dyad which is formed by two amino acid residues like His41 and Cys145 forms in Mpro structure. Also, the Mpro structure comprises three domains, the anti-parallel beta barrels in the first two domains and the alpha-helices arrangement in the third domain. The cleft of the first two domains comprises the His41 and Cys145 residues that are present in the catalytic cavity of SARS-CoV-2-Mpro (Figure 2).

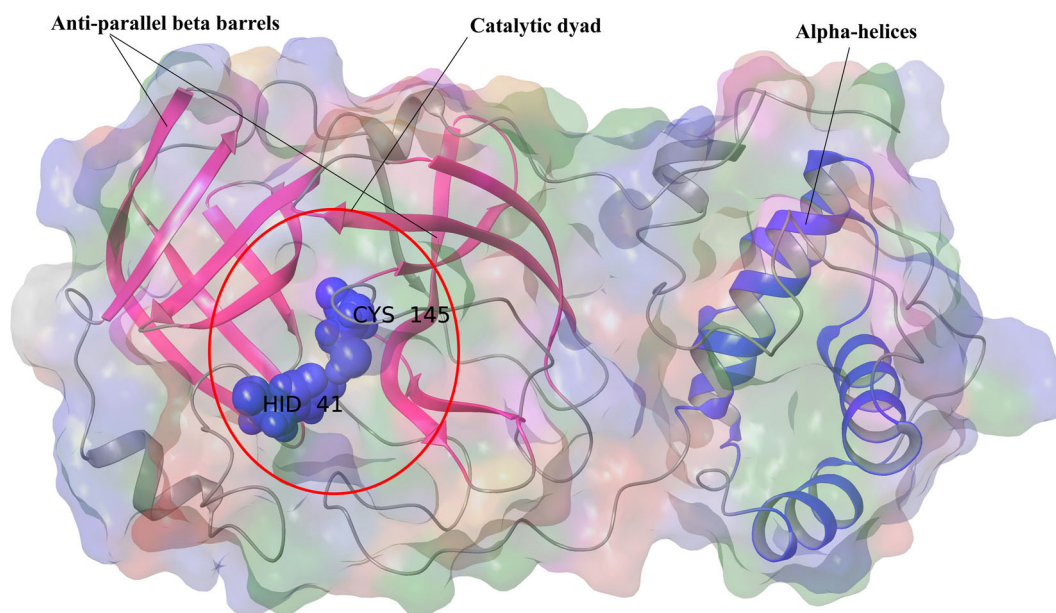
3.2. Molecular docking analysis

The docking energy of biflavonoid compounds along with crystal ligand i.e. N3 and their complete interaction studies is summarized in Table 2. The intermolecular interaction between docked biflavonoid compounds and Mpro was visualized by using Maestro software. The docking analysis suggests that the compound Amentoflavone has a strong binding affinity (−27.0441 kcal/mol) towards Mpro.

Figure 3(a) shows Amentoflavone creates five hydrogen bonds and one aromatic hydrogen binding with Mpro catalytic domain. Amentoflavone binds with Thr26 residues by creating two hydrogen bonds at 1.86 Å and 1.99 Å distances. Also, Asn142, His163, Glu166 involved in the formation of hydrogen bonds with Amentoflavone at 2.08 Å, 1.82 Å, and 2.23 Å bond distances. Glu166 also makes the aromatic hydrogen bond with Amentoflavone at bond distance of 2.59 Å.

Similarly, the second lead compound Agathisflavone is shown to interact with Mpro by forming hydrogen bonds as well as aromatic hydrogen bonds (Figure 3b). The nonpolar residues Phe140 forms hydrogen bonds and aromatic hydrogen bonds with Agathisflavone with a 2.00 Å and 1.98 Å bond distance respectively. Also, the three hydrogen bonds were seen by Gly143, His164 and Gln192 residues and the amino acid Leu141 forms another aromatic hydrogen bonding with Agathisflavone at 2.51 Å bond distance.

In the case of Robustaflavone and Rhusflavanone compounds, the binding affinity towards SARS-CoV-2-Mpro was more similar to −23.6106 kcal/mol and −23.3624 kcal/mol, respectively. The intermolecular interaction analysis was shown in Table 1. Figure 4(a) shows the binding pose of Robustaflavone in the Mpro binding pocket. This binding pattern shows that residues Thr26 are tightly bound with



3D Crystal Structure of SARS-CoV-2 M^{pro} (PDB ID:6LU7)

Figure 2. The 3D structure of SARS-CoV-2 Mpro. The first two domains contain anti-parallel beta barrels shown in pink ribbon, catalytic dyad formed by the residues His41 and Cys145 presented in blue CPK representation and the alpha helices shown in blue color.

Table 2. The intermolecular interactions of *R. succedanea* biflavonoids with SARS-CoV-2-Mpro.

Biflavonoids	PubChem CID	Binding energy (kcal/mol)	Interacting residues	Bond type	Bond distance (Å)
Amentoflavone	5281600	−27.0441	Thr26	2HB	1.86, 1.99
			Asn142	HB	2.08
			His163	HB	1.82
			Glu166	HB	2.23
			Glu166	Ar-HB	2.59
Agathisflavone	5281599	−25.8761	Phe140	HB	2.00
			Phe140	Ar-HB	1.98
			Leu141	Ar-HB	2.51
			Gly143	HB	1.63
			His164	HB	1.85
			Gln192	HB	1.62
Robustaflavone	5281694	−23.6106	Thr26	2HB	1.60, 1.80
			Asn142	HB	2.01
			His163	HB	1.76
			Ser144	Ar-HB	2.49
Rhusflavanone	466314	−23.3624	Gly143	HB	1.75
			Glu166	HB	1.69
			Glu166	Ar-HB	1.85
			Gln189	3HB	1.65, 1.90, 2.00
			Thr190	Ar-HB	2.64
			Asn142	Ar-HB	2.41
Hinokiflavone	5281627	−20.3386	Thr24	HB	1.60
			Thr24	Ar-HB	2.16
			Gly143	HB	1.66
			Glu166	Ar-HB	2.11
			Gln189	HB	1.88
			Gln192	HB	2.23
Succedaneafavanone	12114301	−19.4708	Thr26	HB	2.20
			Thr24	Ar-HB	2.63
			Phe140	HB	1.79
			Asn142	Ar-HB	2.44
			Gly143	HB	1.38
			Ser144	HB	2.19
			Glu166	Ar-HB	1.96
Crystal Ligand (N3) Mpro	PDB ID: 6LU7	−18.5693	Gly143	HB	2.01
			Gln189	2HB	2.04, 2.04
			Glu166	2HB	1.82, 1.89
			His164	HB	2.29
			Phe140	Ar-HB	1.70

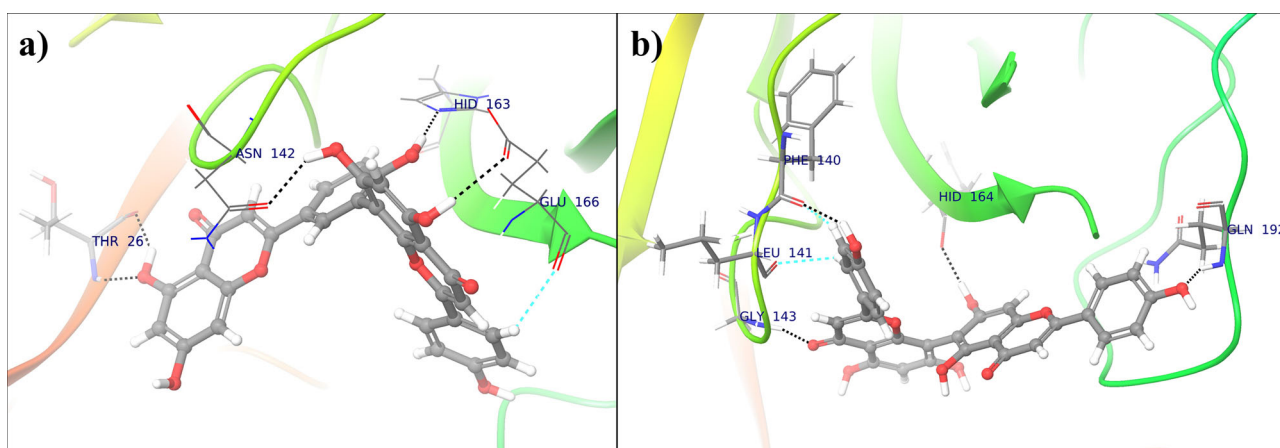


Figure 3. Intermolecular interaction and binding pose of (a) Amentoflavone and (b) Agathisflavone within the binding cavity of Mpro. The crystal structure of Mpro represented as ribbon form, interacting amino acids shown in the tube model and respective bound ligand shown as ball and stick model. The black and blue dotted line represents hydrogen bond and aromatic hydrogen bond interactions, respectively.

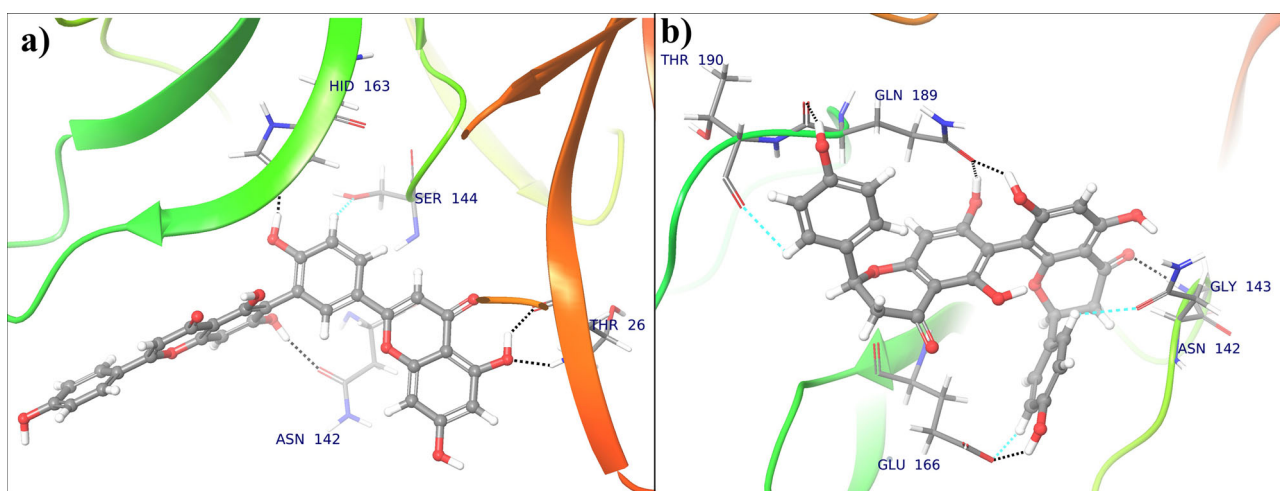


Figure 4. Intermolecular interaction and binding pose of (a) Robustaflavone and (b) Rhusflavanone with Mpro crystal structure. The crystal structure of Mpro is represented in ribbon form, amino acids shown in the tube model and respective bound ligand shown as ball and stick model. The black and blue dotted line represents hydrogen bond and aromatic hydrogen bond interactions, respectively.

Robustaflavone by forming strong two hydrogen bonds. Also, the residues Asn142, His163 and Ser144 form hydrogen bonds and aromatic hydrogen bond with Mpro. **Figure 4(b)** shows the interaction between Rhusflavanone and Mpro. The compound Rhusflavanone interacted with Mpro by forming five hydrogen bonds and three aromatic hydrogen bonds. This binding is mainly due to the amino acid residues like Asn142, Gly143, Glu166, Gln189, and Thr190 which are present in the Mpro binding cavity (Chen et al., 2020; Bzówka et al., 2020).

The lead compound Hinokiflavone was observed to bind with SARS-CoV-2-Mpro with docking energy of -20.3386 . **Figure 5(a)** represents the docked conformation of Hinokiflavone within the binding cavity of Mpro. Two types of bonds (hydrogen bond and aromatic hydrogen bond) are formed by Thr24 with Hinokiflavone. Also, the residues like Gly143, Glu166, Gln189, and Gln192 stabilizes the Hinokiflavone-SARS-CoV-2 complex by forming hydrogen bonds as well as aromatic hydrogen bond to the Hinokiflavone compound. The Succedaneafavanone-Mpro complex showed in **Figure 5(b)** having -19.4708 kcal/mol docking energy. It also forms the four hydrogen bonds and

three aromatic hydrogen bonds with Mpro. The residues Thr26, Phe140, Gly143 and Ser144 are involved in hydrogen bonding at 2.20 Å, 1.79 Å, 1.38 Å, and 2.19 Å a bond distances respectively. Also, this complex is stabilized by aromatic hydrogen bonds between residues Thr24, Asn142, Glu166 and Succedaneafavanone compound. From this docking analysis, we can interpret that these biflavonoids have a binding affinity towards SARS-CoV2-Mpro and Thr26, Asn142, Gly143, Ser144 and Glu166 are the crucial amino acids in Mpro for the binding of biflavonoid compounds. Also, the reported lead compounds having a more binding affinity than the crystal (in-bound) ligand, i.e. N3. Previous computational docking reports and our recent report on Mpro from SARS-CoV-2 demonstrated the interaction of similar key amino acids in the binding cavity (Lakshmi et al., 2020; Lokhande et al., 2020b).

These biflavonoids from *R. succedanea* have been recorded as promising antiviral agents against HIV-1 reverse transcriptase which mitigate the HIV-1 activity in infected primary human lymphocytes (PBM) (Lin et al., 1997). In addition, Robustaflavone has been reported to acts as a potent inhibitor of Hepatitis B Virus (HBV) replication in human

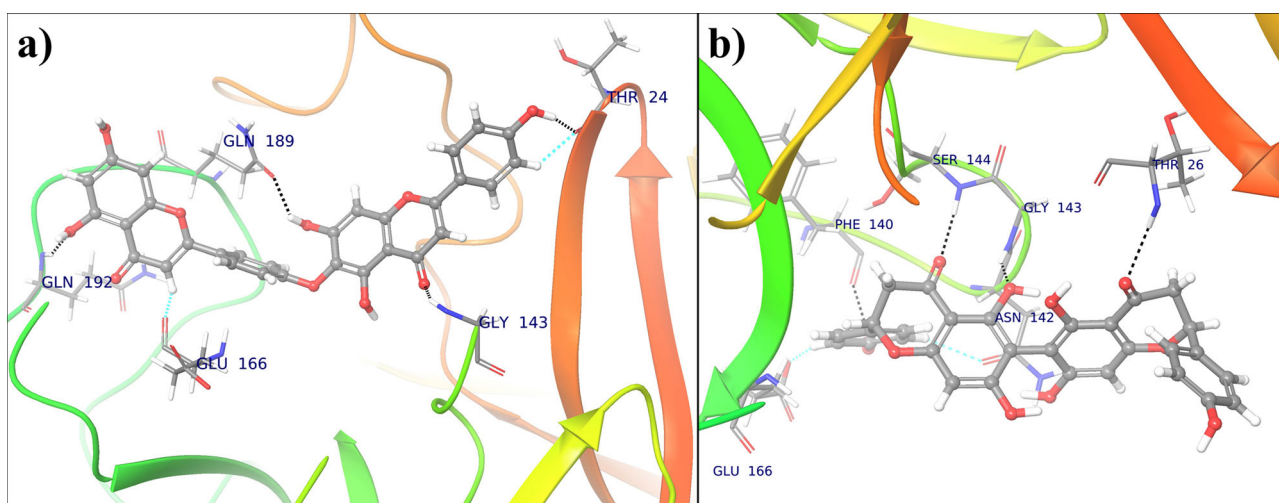


Figure 5. Intermolecular interaction and binding pose of (a) Hinokiflavone and (b) Sucedaneaflavanone with the crystal structure of Mpro. The crystal structure of Mpro is represented in ribbon form, amino acid residues shown in the tube model and respective bound ligand shown as ball and stick model. The black and blue dotted line represents hydrogen bond and aromatic hydrogen bond interactions, respectively.

hepatoblastoma 2.2.15 cells (Zembower et al., 1998). The potential inhibitory activities of these biflavonoids against a large number of human infected viruses such as respiratory viruses (influenza A and B, Para-influenza type 3, respiratory syncytial, type 5 Adenovirus and Measles), Herpes Simplex Virus (HSV types 1 and 2) and Varicella Zoster Virus (VZV) were investigated earlier (Lin et al., 1999). Besides, herbal medicinal plant-derived flavonoids such as herbacetin, rhoifolin and pectolarin were found to efficiently block the SARS-CoV 3CLpro enzymatic activity (Jo et al., 2020). Altogether, the reported antiviral properties of *R. succedanea* biflavonoids prompted our research interest to predict its inhibitory activity against SARS-CoV-2.

3.3. Dynamic behavior of biflavonoids with SARS-CoV-2-Mpro

The SARS-CoV-2-Mpro crystal structure was considered rigid through the FlexX protein-ligand docking calculations, to acquire a more realistic model of interaction patterns between biflavonoids and Mpro, the docked complexes were solvated in explicit solvent (TIP3 water model) PBC box for 100 ns simulation. The time-evolutionary structural changes in the SARS-CoV-2 Mpro after biflavonoid binding were determined in terms of RMSD and RMSF. Besides structural changes in the binding site residues also recorded during the 100 ns MD simulation, the average RMSF values of binding site residues were shown in Table 3. The RMSD graphs of the SARS-CoV-2 C- α atoms as shown in Figure 6, illustrate that throughout the 100 ns MD simulation period all complexes of SARS-CoV-2 Mpro and reported biflavonoids were remained in the equilibration state from 1.5 Å to 3.0 Å RMSD. In the simulation of the SARS-CoV-2-Agathisflavone complex, the slight deviation observed in C- α atoms (backbone) during 70 ns to 97 ns, suggest that after binding of Agathisflavone, the SARS-CoV-2 Mpro structure slightly deviate from other complexes.

Also the separate RMSD graph of lead compounds biflavonoids reported as shown in Figure 7 to reveal the

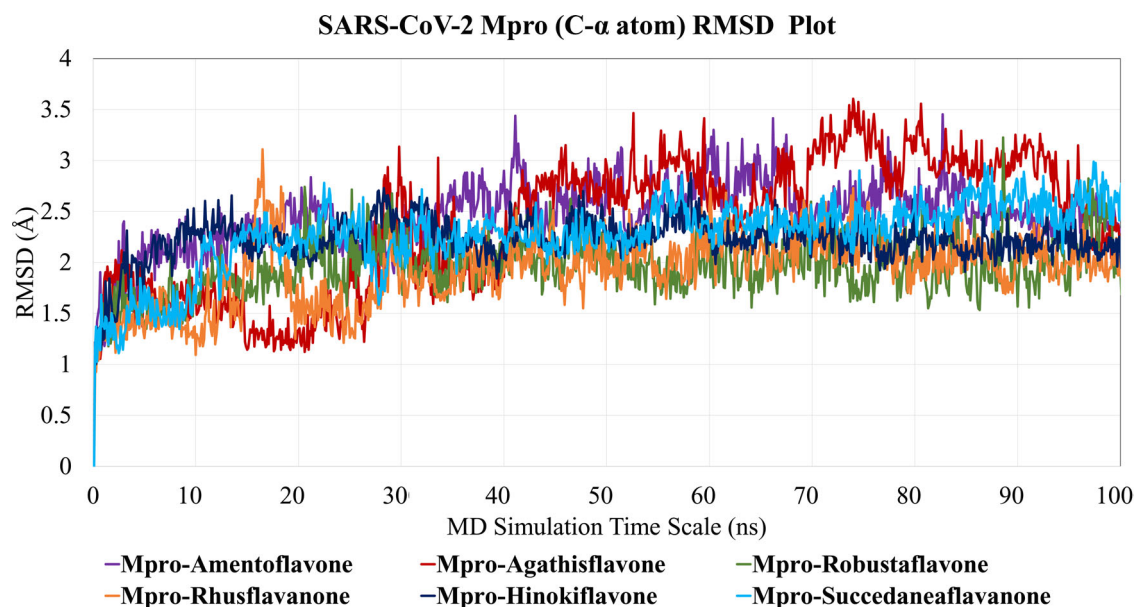
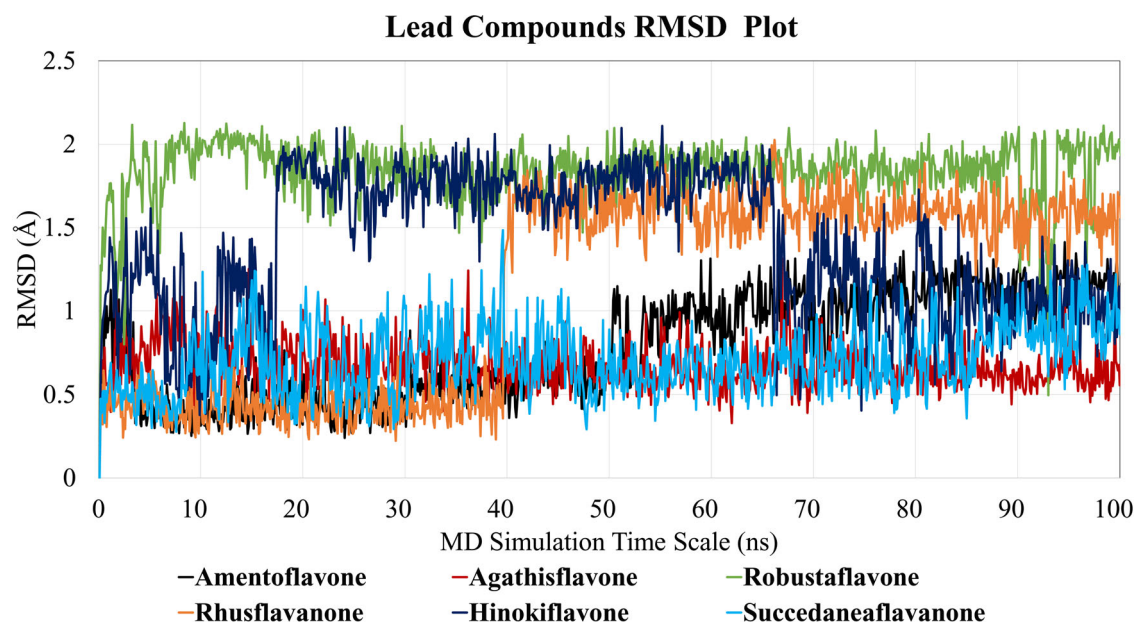
conformational stability and mobility of docked biflavonoids within the binding pocket of SARS-CoV-2-Mpro. From the lead compound RMSD graph (Figure 7), it is clearly noticed that the RMSD values of all the docked biflavonoids are within 2.5 Å, reveal that all the docked biflavonoids are very stable in the binding cavity of Mpro. In the case of Amentoflavone, Agathisflavone and Sucedaneaflavanone the RMSD lies within the 1.5 Å RMSD while Rhusflavanone and Hinokiflavone achieve a different equilibration state in the binding cavity of SARS-CoV-2 Mpro. The Rhusflavanone initially very stable within 0.5 Å RMSD up to 40 ns simulation, afterwards, the Rhusflavanone deviate from 0.5 Å to 1.7 Å within the cavity and maintain the second equilibration state up to 100 ns MD simulation time.

On other hand, Hinokiflavone forms three equilibration state within the cavity, first, equilibration was seen up to 18 ns with RMSD value about 1.5 Å, second equilibration state slightly deviates the Hinokiflavone from 1.5 Å to 2.00 Å RMSD (18–68 ns), afterwards, it again achieves the initial equilibration within the 1.5 Å RMSD. In the case of Robustaflavone, it deviates initially just after the simulation started to 2.0 Å and maintains the conformational stability within the binding cavity. Although Rhusflavanone, Hinokiflavone and Robustaflavone showed different equilibration states, they are not moving from the cavity and able to maintain the stable conformations within the binding pocket of SARS-CoV-2-Mpro during the 100 ns MD simulation.

The RMSF values were calculated to explore the effect of biflavonoids upon the flexibility of SARS-CoV-2 Mpro C- α atoms (Figure 8). The RMSF graph suggests that the fluctuation in the SARS-CoV-2 Mpro C- α atoms is minimum within the RMSF value 2.0 Å when it binds with the reported biflavonoids. In some of the regions, the fluctuation goes up to 3.0 Å, but the fluctuation in the binding site region is very low (Table 3). Overall these results indicate that biflavonoids make the protein-ligand complex more stable throughout the 100 ns MD simulation. Also, we have computed the Radius of gyration. The Radius of gyration (Rg) evaluation is employed to investigate the compactness level and the

Table 3. RMSF values (Å) of the binding site residues of SARS-CoV-2 Mpro upon binding with biflavonoids.

Binding site residues	Amento-flavone	Agathis-flavone	Robusta-flavone	Rhus-flavanone	Hinoki-flavone	Succedanea-flavanone
Thr24	1.57	2.276	1.477	1.774	1.312	1.747
Thr26	1.043	0.837	0.923	1.222	0.807	0.858
Phe140	1.428	1.126	1.256	1.41	0.975	1.567
Leu141	1.638	1.224	1.4	1.573	1.154	1.875
Asn142	1.56	1.219	1.394	1.709	1.184	1.652
Gly143	1.306	0.953	1.122	1.24	0.95	1.157
His163	0.606	0.547	0.702	0.562	0.527	0.606
His164	0.675	0.573	0.733	0.767	0.663	0.683
Glu166	0.879	1.123	0.972	0.787	0.859	1.047
Thr190	2.758	1.39	1.329	1.451	1.334	1.361
Gln192	2.042	1.394	1.342	1.721	1.16	1.271

**Figure 6.** The Root Mean Square Deviation (RMSD) graph of the SARS-CoV-2 Mpro C- α atoms when complexed with biflavonoids during 100 ns time-scale simulation.**Figure 7.** The Root Mean Square Deviation (RMSD) graph for the biflavonoids when complexed with the SARS-CoV-2 Mpro structure during the 100 ns MD simulation.

folding properties of protein structure as well as protein-ligand complex structures. Distribution of atoms from the center of mass computed by the Rg analysis, which resulted in

the compactness of the protein-ligand complex. [Figure S1, supplementary material](#), illustrated that the Radius of gyration for SARS-CoV-2 Mpro structure complexed with

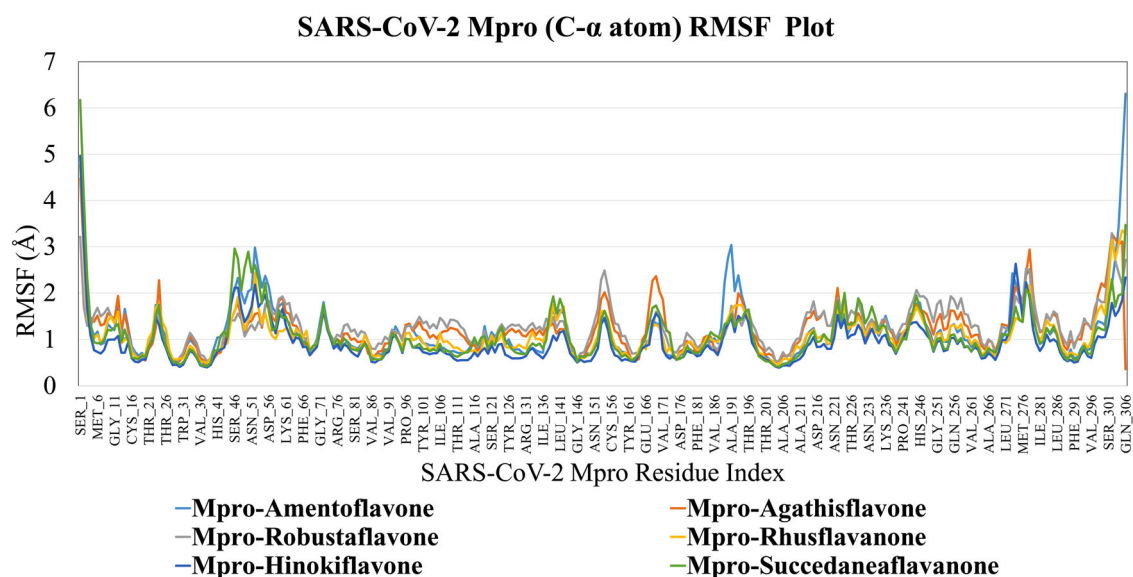


Figure 8. The Root Mean Square Fluctuation (RMSF) graph of the SARS-CoV-2-Mpro C- α atoms when complexed with biflavonoids during the 100 ns MD simulation.

Table 4. The Prime MM/GBSA (ensemble-averaged) binding free energies (kcal/mol) of biflavonoids with SARS-CoV-2 Mpro during the 100 ns MD simulation.

Lead compound complexed with SARS-CoV-2 Mpro	MM/GBSA dG bind (kcal/mol)	MM/GBSA dG bind Coulomb (kcal/mol)	MM/GBSA dG bind Solv GB (kcal/mol)	MM/GBSA dG bind vdW (kcal/mol)	Complex energy (kcal/mol)
Amentoflavone	-72.650 ±15.778	-34.477 ±8.372	27.9036 ±3.797	-46.603 ±9.877	-8846.248 ±68.264
Agathisflavone	-47.773 ±9.993	-14.350 ±5.804	17.788 ±5.918	-33.776 ±9.349	-8830.648 ±95.240
Robustaflavone	-60.157 ±7.745	-19.889 ±8.744	25.519 ±4.634	-45.781 ±6.245	-8812.960 ±53.844
Rhusflavanone	-70.950 ±7.585	-18.877 ±8.251	26.491 ±5.465	-57.145 ±8.594	-8822.949 ±69.059
Hinokiflavone	-87.003 ±10.804	-25.501 ±7.325	24.377 ±2.941	-57.840 ±4.806	-8781.250 ±73.606
Succedaneaflavanone	-71.518 ±9.473	-28.819 ±9.197	28.383 ±5.416	-51.597 ±4.479	-8838.326 ±82.159

reported biflavonoids least fluctuation within 2.2 nm (22 Å) to 2.3 nm (23 Å). Thus, the SARS-CoV-2 Mpro-biflavonoids complexes are thermodynamically stable and more compact during 100 ns MD simulation.

3.4. Prime MM/GBSA binding free energies of biflavonoids-SARS-CoV-2-Mpro complex

The MM/GBSA has been studied to compute the binding free energies i.e. ΔG Bind that affirms the outcomes in terms of solvation, VDW, and hydrophobic, VDW components. The docked biflavonoid, complexed with SARS-CoV-2 Mpro structure (PDB ID: 6LU7) were subjected to binding free energy (Prime MM/GBSA) calculation for a 100 ns time-scale molecular dynamic simulation. The computed Prime MM/GBSA energies of the six biflavonoids complexed with SARS-CoV-2 Mpro were described in Table 4. The stability of the receptor-ligand complex is considered strong when the computed values of binding free energies are more negative (Lokhande et al., 2020b).

The obtained binding free energies of all reported biflavonoids with SARS-CoV-2 Mpro have the binding free energies

less than -70 kcal/mol except biflavonoid like Robustaflavone. In the case of Robustaflavone, the resulting binding free energy is -60.57 kcal/mol suggesting that it make a slightly weaker complex with SARS-CoV-2 Mpro than the other biflavonoids. However, other biflavonoids shows the favorable Prime MM/GBSA binding free energy after binding with Mpro of SARS-CoV-2, signifying that reported biflavonoids forms a stable and strong binding with the SARS-CoV-2-Mpro and these complexes are thermodynamically favorable.

3.5. Binding pocket properties of SARS-CoV-2-Mpro

The generation of the hydrophobic and hydrophilic surface on structure enlightens the binding pocket properties of the SARS-CoV-2-Mpro receptor, reveals the preferred ligands atoms in terms of their physicochemical properties that can be fitted well in the region of binding site with minimum steric clashes. Figure 9 illustrates that the hydrophobic/hydrophilic surface and all docked biflavonoid compounds within the Mpro binding cavity. Interestingly, the binding cavity of SARS-CoV-2-Mpro is occupied by both the region,

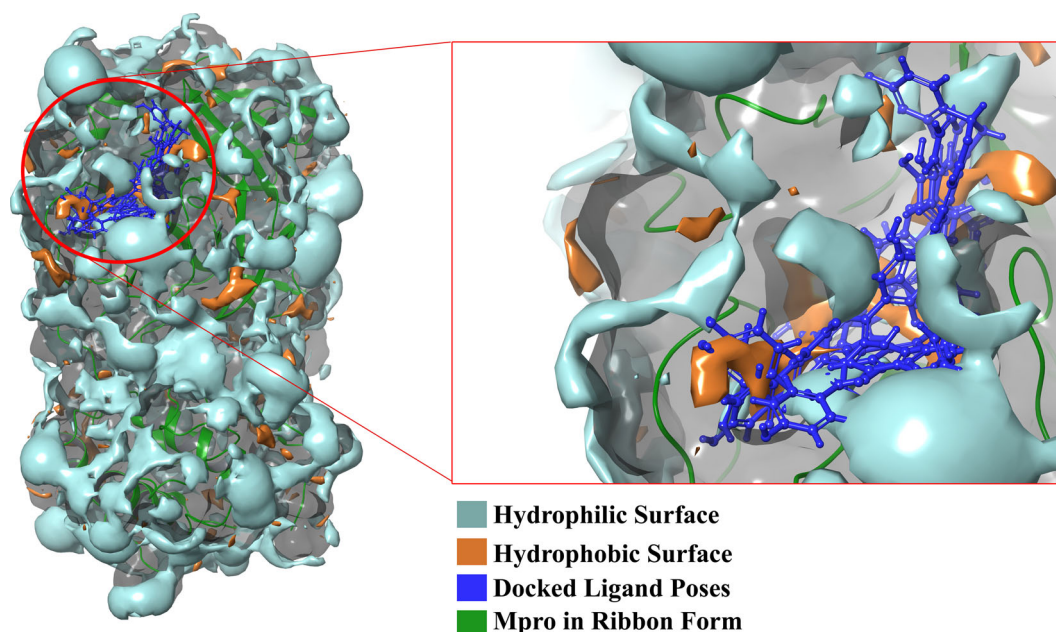


Figure 9. Graphical illustration of the SARS-CoV-2-Mpro surface, occupied by the hydrophilic and hydrophobic surface. The docked ligand poses shown in the ball and stick model with blue color, the secondary structure of the receptor is presented in ribbon form with green color. The hydrophilic and hydrophobic surface area is shown in turquoise and orange color, respectively.

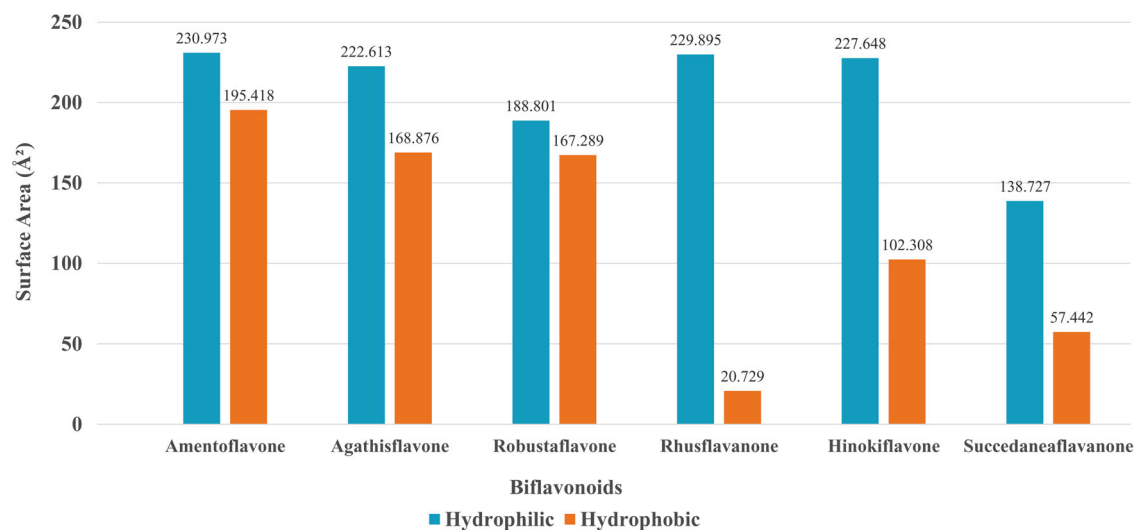


Figure 10. The hydrophilic and hydrophobic surface area is formed by docked biflavonoids within the SARS-CoV-2-Mpro.

suggesting that the ligand having hydrophobic as well as hydrophilic the functional group atoms are also known as nonpolar molecules and polar atoms.

The total surface area of SARS-CoV-2-Mpro was found to be 11,545.574 Å², also in Figure 10, we have reported the hydrophobic and hydrophilic surface area of docked biflavonoid poses to know which ligand atoms properties are most favorable for the binding affinity. Figure 11 illustrates that the comparative hydrophobic and hydrophilic surface area shows that the compound Amentoflavone having a more or less similar surface area in context with hydrophobic (230.973 Å²) and hydrophilic (195.418 Å²) surface area on it and it was shown higher binding affinity (−27.0441 kcal/mol) toward the SARS-CoV-2-Mpro as compare to other biflavonoids. From this study, we can conclude that the structures

having both the functionality are favorable to binds with SARS-CoV-2-Mpro and exert its inhibitory effect. Also, we have computed the pharmacokinetic (ADME) properties for reported biflavonoids using the QikProp application of Schrodinger software. All the reported bioflavonoids having the Bioavailability score ranges from 0.17 to 0.55 and Synthetic accessibility in between 4.05 and 4.66, this study help to design biflavonoids derivatives with greater potency.

4. Conclusion

At present, there is no any promising drug or vaccine against SARS-CoV-2. Chemical drugs are not always suitable for human health due to their adverse effect. Therefore, there is

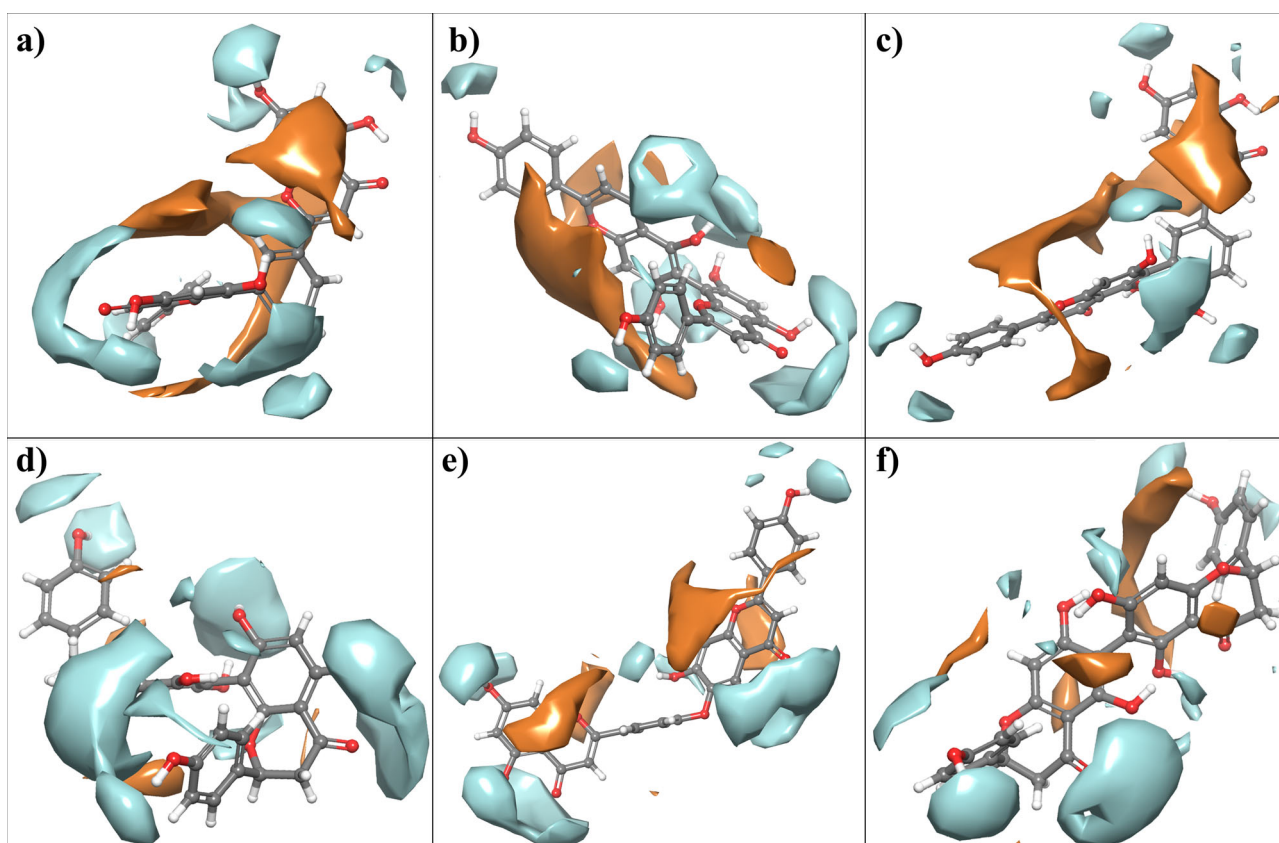


Figure 11. Graphical illustration of the hydrophilic and hydrophobic surface formed by docked biflavonoid within the SARS-CoV-2-Mpro and shown in turquoise and orange color, respectively.

an urgent need to search for a non-toxic and novel drug against this deadly virus. Natural compounds have received immense attention due to their wide range of applications in human health and diseases without causing any side effects. Molecular docking is an important tool for drug discovery as this method provides effective screening in a short time for probable drugs. In this study, we hypothesized that natural biflavonoids could act as promising inhibitors to SARS-CoV-2 Mpro. To investigate this, we employed a molecular docking tool against SARS-CoV-2 Mpro. Binding energy and affinities between biflavonoids and the Mpro enzyme suggest that all six biflavonoids demonstrate promising interaction with the catalytic site of this Mpro enzyme. Comparative molecular dynamic simulations were carried out to reveal the effect dynamic behavior of SARS-CoV-2 Mpro upon binding of biflavonoids. One interesting finding revealed from MD studies is that the RMSD values for the SARS-CoV-2 Mpro C- α atoms are within 2.5 Å suggest that the reported biflavonoids can make a strong complex with SARS-CoV-2 Mpro. Also, the reported RMSF values for the binding site residues suggest that the minimum fluctuations occur when biflavonoids binds in the binding pocket SARS-CoV-2 Mpro. The computed Prime MM/GBSA binding free energies are thermodynamically favorable. In addition, hydrophobic and hydrophilic surface mapping on the SARS-CoV-2 Mpro structure as well as biflavonoids were exploited for the further lead optimization process. Future *in vitro* and clinical studies against SARS-CoV-2 should be considered to get fundamental activities and mechanisms of these biflavonoids.

Acknowledgements

The authors are thankful to Dr. D. Y. Patil Biotechnology and Bioinformatics Institute, Dr. D. Y. Patil Vidyapeeth, Tathawade, Pune, for providing the necessary facilities and infrastructure to carry out this work. The authors also acknowledge the Department of Science and Technology-Science and Engineering Research Board (DST-SERB), Govt. of India, New Delhi, (File Number: YSS/2015/002035) for Optimized Supercomputer facility for dynamics calculations. Kiran Bharat Lokhande acknowledges the Indian Council of Medical Research (ICMR), New Delhi, for Senior Research Fellowship (Project ID: 2019-3458; File: ISRM/11(54)/2019).

Funding

This work received funding from Dr. D. Y. Patil Vidyapeeth, Pune (DPU/421/2018).

ORCID

Sarika Pawar  <http://orcid.org/0000-0002-9990-5234>

References

- Alonso, H., Bliznyuk, A. A. , & Gready, J. E. (2006). Combining docking and molecular dynamic simulations in drug design. *Medicinal Research Reviews*, 26(5), 531–568. <https://doi.org/10.1002/med.20067.16758486>
- Amin, S. A., Banerjee, S., Ghosh, K., Gayen, S., & Jha, T. (2020). Protease targeted COVID-19 drug discovery and its challenges: Insight into viral main protease (Mpro) and papain-like protease (PLpro) inhibitors.

- Bioorganic & Medicinal Chemistry*, 115860. Advance online publication. <https://doi.org/10.1016/j.bmc.2020.115860>
- Amin, S. A., & Jha, T. (2020). Fight against novel coronavirus: A perspective of medicinal chemists. *European Journal of Medicinal Chemistry*, 201, 112559. <https://doi.org/10.1016/j.ejmech.2020.112559>
- Anand, K., Palm, G. J., Mesters, J. R., Siddell, S. G., Ziebuhr, J., & Hilgenfeld, R. (2002). Structure of coronavirus main proteinase reveals combination of a chymotrypsin fold with an extra alpha-helical domain. *The EMBO Journal*, 21(13), 3213–3224. <https://doi.org/10.1093/emboj/cdf327>
- Bzówka, M., Mitusińska, K., Raczynska, A., Samol, A., Tuszyński, J. A., & Góra, A. (2020). Structural and Evolutionary Analysis Indicate That the SARS-CoV-2 Mpro Is a Challenging Target for Small-Molecule Inhibitor Design. *International Journal of Molecular Sciences*, 21(9), 3099. <https://doi.org/10.3390/ijms21093099>
- Cazarolli, L., Zanatta, L., Alberton, E., Bonorino Figueiredo, M. S., Folador, P., Damazio, R., Pizzolatti, M. G., & Barreto Silva, F. R. (2008). Flavonoids: Prospective drug candidates. *Mini Reviews in Medicinal Chemistry*, 8(13), 1429–1440. <https://doi.org/10.2174/138955708786369564>
- Chen, Y. W., Yiu, B., & Wong, K.-Y. (2020). Prediction of the SARS-CoV-2 (2019-nCoV) 3C-like protease (3CLpro) structure: virtual screening reveals velpatasvir, ledipasvir, and other drug repurposing candidates. *F1000Research*, 9, 129. <https://doi.org/10.12688/f1000research.22457.1>
- Chen, F. C., & Lin, Y. M. (1975). Succedaneoflavanone—a new 6,6"-binaringenin from *Rhus succedanea*. *Phytochemistry*, 14(7), 1644–1647. [https://doi.org/10.1016/0031-9422\(75\)85371-4](https://doi.org/10.1016/0031-9422(75)85371-4)
- Chen, F.-C., & Lin, Y.-M. (1976). Rhusflavanone, a new biflavanone from the seeds of wax-tree. *Journal of the Chemical Society, Perkin Transactions 1*, 1(1), 98. <https://doi.org/10.1039/p19760000098>
- Chen, Y. W., Yiu, C.-P. B., & Wong, K.-Y. (2020). Prediction of the SARS-CoV-2 (2019-nCoV) 3C-like protease (3CLpro) structure: Virtual screening reveals velpatasvir, ledipasvir, and other drug repurposing candidates. *F1000Research*, 9, 129. <https://doi.org/10.12688/f1000research.22457.1>
- Costa, A. N., de Sá, É. R. A., Bezerra, R. D. S., Souza, J. L., & Lima, F. D. C. A. (2020). Constituents of buriti oil (*Mauritia flexuosa* L.) like inhibitors of the SARS-Coronavirus main peptidase: An investigation by docking and molecular dynamics. *Journal of Biomolecular Structure and Dynamics*, 22, 1–8. <https://doi.org/10.1080/07391102.2020.1778538>
- Das, S., Sarmah, S., Lyndem, S., & Singha Roy, A. (2020). An investigation into the identification of potential inhibitors of SARS-CoV-2 main protease using molecular docking study. *Journal of Biomolecular Structure and Dynamics*, 1–11. Advance online publication. <https://doi.org/10.1080/07391102.2020.1763201>
- De Vivo, M., Masetti, M., Bottegoni, G., & Cavalli, A. (2016). Role of Molecular Dynamics and Related Methods in Drug Discovery. *Journal of Medicinal Chemistry*, 59(9), 4035–4061. <https://doi.org/10.1021/acs.jmedchem.5b01684>
- Dong, L., Hu, S., & Gao, J. (2020). Discovering drugs to treat coronavirus disease 2019 (COVID-19). *Drug Discoveries & Therapeutics*, 14(1), 58–60. <https://doi.org/10.5582/ddt.2020.01012>
- Enmozhi, S. K., Raja, K., Sebastine, I., & Joseph, J. (2020). Andrographolide as a potential inhibitor of SARS-CoV-2 main protease: An in silico approach. *Journal of Biomolecular Structure and Dynamics*, 0, 1–7. Advance online publication. <https://doi.org/10.1080/07391102.2020.1760136>
- Etaware, P. M. (2020). Medicinal plants, synthetic drugs or clinical therapy: The safest option against the pandemic covid-19 coronavirus. *Pharmacology and Alternative Medicine Academic Journal*, 5(3), 1–13.
- Fa-Ching, C., Yuh-Meei, L., & Chi-Ming, L. (1974). Biflavonyls from drupes of *Rhus succedanea*. *Phytochemistry*, 13(1), 276–278. [https://doi.org/10.1016/S0031-9422\(00\)91311-6](https://doi.org/10.1016/S0031-9422(00)91311-6)
- Ghosh, R., Chakraborty, A., Biswas, A., & Chowdhuri, S. (2020). Evaluation of green tea polyphenols as novel corona virus (SARS CoV-2) main protease (Mpro) inhibitors – an in silico docking and molecular dynamics simulation study. *Journal of Biomolecular Structure and Dynamics*, 0, 1–13. Advance online publication. <https://doi.org/10.1080/07391102.2020.1779818>
- Goyal, B., & Goyal, D. (2020). Targeting the dimerization of the main protease of coronaviruses: A potential broad-spectrum therapeutic strategy. *ACS Combinatorial Science*, 22(6), 297–305. <https://doi.org/10.1021/acscombsci.0c00058>
- Harborne, J. B., & Williams, C. A. (2000). Advances in flavonoid research since 1992. *Phytochemistry*, 55(6), 481–504. [https://doi.org/10.1016/S0031-9422\(00\)00235-1](https://doi.org/10.1016/S0031-9422(00)00235-1)
- Havranek, B., & Islam, S. M. (2020). An in silico approach for identification of novel inhibitors as potential therapeutics targeting COVID-19 main protease. *Journal of Biomolecular Structure and Dynamics*, 0, 1–12. Advance online publication. <https://doi.org/10.1080/07391102.2020.1776158>
- Jacobson, M. P., Pincus, D. L., Rapp, C. S., Day, T. J., Honig, B., Shaw, D. E., & Friesner, R. A. (2004). A hierarchical approach to all-atom protein loop prediction. *Proteins*, 55(2), 351–367. <https://doi.org/10.1002/prot.10613>
- Jin, Z., Du, X., Xu, Y., Deng, Y., Liu, M., Zhao, Y., Zhang, B., Li, X., Zhang, L., Peng, C., Duan, Y., Yu, J. L., Yang, K., Liu, F., Jiang, R., Yang, X., You, T., Liu, X., Yang, X., & Yang, H. (2020). Structure of Mpro from SARS-CoV-2 and discovery of its inhibitors. *Nature*, 582(7811), 289–293. <https://doi.org/10.1038/s41586-020-2223-y>
- Jo, S., Kim, S., Shin, D. H., & Kim, M. S. (2020). Inhibition of SARS-CoV 3CL protease by flavonoids. *Journal of Enzyme Inhibition and Medicinal Chemistry*, 35(1), 145–151. <https://doi.org/10.1080/14756366.2019.1690480>
- Joshi, R. S., Jagdale, S. S., Bansode, S. B., Shankar, S. S., Tellis, M. B., Pandya, V. K., Chugh, A., Giri, A. P., & Kulkarni, M. J. (2020). Discovery of potential multi-target-directed ligands by targeting host-specific SARS-CoV-2 structurally conserved main protease. *Journal of Biomolecular Structure and Dynamics*, 1–16. Advance online publication. <https://doi.org/10.1080/07391102.2020.1760137>
- Khan, S. A., Barkatullah, & Khan, B. (2020). Anatomy, micromorphology, and physicochemical analysis of *Rhus succedanea* var. himalaica root. *Microscopy Research and Technique*, 83(4), 424–435. <https://doi.org/10.1002/jemt.23430>
- Khan, S. A., Ibrar, M., & Barkatullah. (2016). Pharmacognostic evaluation of the leaf OF *Rhus succedanea* Var. Himalaica. *J. D Hooker. African Journal of Traditional, Complementary and Alternative Medicines*, 13(6), 107–120. <https://doi.org/10.21010/ajtcam.v13i6.16>
- Kim, D. H., Lee, S. J., Oh, D. S., Lee, I. D., Eom, J. S., Park, H. Y., Choi, S. H., & Lee, S. S. (2018). In vitro evaluation of *Rhus succedanea* extracts for ruminants. *Asian-Australasian Journal of Animal Sciences*, 31(10), 1635–1642. <https://doi.org/10.5713/ajas.18.0045>
- Kumar, V., Dhanjal, J. K., Kaul, S. C., Wadhwa, R., & Sundar, D. (2020). Withanone and caffeic acid phenethyl ester are predicted to interact with main protease (Mpro) of SARS-CoV-2 and inhibit its activity. *Journal of Biomolecular Structure and Dynamics*, 1–13. Advance online publication. <https://doi.org/10.1080/07391102.2020.1772108>
- Lakshmi, S. A., Shafreen, R. M. B., Priya, A., & Shunmugiah, K. P. (2020). Ethnomedicines of Indian origin for combating COVID-19 infection by hampering the viral replication: Using structure-based drug discovery approach. *Journal of Biomolecular Structure and Dynamics*, 1–16. Advance online publication. <https://doi.org/10.1080/07391102.2020.1778537>
- LeadIT version 2.3.2; BioSolveIT. (2017). GmbH, Sankt Augustin, Germany, www.biosolveit.de/LeadIT.
- Li, Q., & Kang, C. (2020). Progress in developing inhibitors of SARS-CoV-2 3C-like protease. *Microorganisms*, 8(8), 1250. <https://doi.org/10.3390/microorganisms8081250>
- Lin, Y.-M., Anderson, H., Flavin, M. T., Pai, Y.-H. S., Mata-Greenwood, E., Pengsuparp, T., Pezzuto, J. M., Schinazi, R. F., Hughes, S. H., & Chen, F.-C. (1997). In vitro anti-HIV activity of biflavonoids isolated from *Rhus succedanea* and *Garcinia multiflora*. *Journal of Natural Products*, 60(9), 884–888. <https://doi.org/10.1021/np9700275>
- Lin, Y.-M., Flavin, M. T., Schure, R., Chen, F.-C., Sidwell, R., Barnard, D. I., Huffmann, J. H., & Kern, E. R. (1999). Antiviral activities of biflavonoids. *Planta Medica*, 65(2), 120–125. <https://doi.org/10.1055/s-1999-13971>
- Lokhande, K. B., Ballav, S., Yadav, R. S., Swamy, K. V., & Basu, S. (2020a). Probing intermolecular interactions and binding stability of kaempferol, quercetin and resveratrol derivatives with PPAR- γ : Docking, molecular dynamics and MM/GBSA approach to reveal potent PPAR- γ agonist against cancer. *Journal of Biomolecular Structure &*

- Dynamics*, 1–11. Advance online publication. <https://doi.org/10.1080/07391102.2020.1820380>
- Lokhande, K. B., Doiphode, S., Vyas, R., & Swamy, K. V. (2020b). Molecular docking and simulation studies on SARS-CoV-2 Mpro reveals Mitoxantrone, Leucovorin, Birinapant, and Dynasore as potent drugs against COVID-19. *Journal of Biomolecular Structure and Dynamics*, 1–12. Advance online publication. <https://doi.org/10.1080/07391102.2020.1805019>
- Lokhande, K. B., Nagar, S., & Swamy, K. V. (2019). Molecular interaction studies of Deguelin and its derivatives with Cyclin D1 and Cyclin E in cancer cell signaling pathway: The computational approach. *Scientific Reports*, 9(1), 1778. <https://doi.org/10.1038/s41598-018-38332-6>
- Marinho, E. M., Batista de Andrade Neto, J., Silva, J., Rocha da Silva, C., Cavalcanti, B. C., Marinho, E. S., & Nobre Júnior, H. V. (2020). Virtual screening based on molecular docking of possible inhibitors of Covid-19 main protease. *Microbial Pathogenesis*, 148, 104365. <https://doi.org/10.1016/j.micpath.2020.104365>
- Meng, X. Y., Zhang, H. X., Mezei, M., & Cui, M. (2011). Molecular docking: A powerful approach for structure-based drug discovery. *Current Computer-Aided Drug Design*, 7(2), 146–157. <https://doi.org/10.2174/157340911795677602>
- Pandeya, K. B., Ganeshpurkar, A., & Mishra, M. K. (2020). Natural RNA dependent RNA polymerase inhibitors: Molecular docking studies of some biologically active alkaloids of *Argemone mexicana*. *Medical Hypotheses*, 144, 109905. <https://doi.org/10.1016/j.mehy.2020.109905>
- Sharma, N., Muthamilarasan, M., Prasad, A., & Prasad, M. (2020). Genomics approaches to synthesize plant-based biomolecules for therapeutic applications to combat SARS-CoV-2. *Genomics*, 112(6), 4322–4331. <https://doi.org/10.1016/j.ygeno.2020.07.033>
- Shrestha, S., Subaramaiha, S. R., Subbaiah, S. G. P., Eshwarappa, R. S. B., & Lakkappa, D. B. (2013). Evaluating the antimicrobial activity of methanolic extract of *Rhus succedanea* leaf gall. *Bioimpacts: Bi*, 3(4), 195–198. <https://doi.org/10.5681/bi.2013.035>
- Siddiqui, A. J., Danciu, C., Ashraf, S. A., Moin, A., Singh, R., Alreshidi, M., Patel, M., Jahan, S., Kumar, S., Alkhinjar, M. I. M., Badraoui, R., Snoussi, M., & Adnan, M. (2020a). Plants-derived biomolecules as potent antiviral phytomedicines: New insights on ethnobotanical evidences against coronaviruses. *Plants*, 9(9), 1244. <https://doi.org/10.3390/plants9091244>
- Siddiqui, A. J., Jahan, S., Ashraf, S. A., Alreshidi, M., Ashraf, M. S., Patel, M., Snoussi, M., Singh, R., & Adnan, M. (2020b). Current status and strategic possibilities on potential use of combinational drug therapy against COVID-19 caused by SARS-CoV-2. *Journal of Biomolecular Structure and Dynamics*, 1–14. Advance online publication. <https://doi.org/10.1080/07391102.2020.1802345>
- Surti, M., Patel, M., Adnan, M., Moin, A., Ashraf, S. A., Siddiqui, A. J., Snoussi, M., Deshpande, S., & Reddy, M. N. (2020). Ilimaquinone (marine sponge metabolite) as a novel inhibitor of SARS-CoV-2 key target proteins in comparison with suggested COVID-19 drugs: Designing, docking and molecular dynamics simulation study. *RSC Advances*, 10(62), 37707–37720. <https://doi.org/10.1039/D0RA06379G>
- Ullrich, S., & Nitsche, C. (2020). The SARS-CoV-2 main protease as drug target. *Bioorganic & Medicinal Chemistry Letters*, 30(17), 127377. <https://doi.org/10.1016/j.bmcl.2020.127377>
- Umesh, K. D., Selvaraj, C., Singh, S. K., & Dubey, V. K. (2020). Identification of new anti-nCoV drug chemical compounds from Indian spices exploiting SARS-CoV-2 main protease as target. *Journal of Biomolecular Structure and Dynamics*, 1–9. Advance online publication. <https://doi.org/10.1080/07391102.2020.1763202>
- Wang, G., & Zhu, W. (2016). Molecular docking for drug discovery and development: a widely used approach but far from perfect. *Future Medicinal Chemistry*, 8(14), 1707–1710. <https://doi.org/10.4155/fmc-2016-0143>
- World Health Organization. (2020). Coronavirus disease (COVID-19) pandemic 2020. World Health Organization. <https://www.who.int/emergencies/diseases/novel-coronavirus-2019>
- Wu, P.-L., Lin, S.-B., Huang, C.-P., & Chiou, R. Y. Y. (2002). Antioxidative and cytotoxic compounds extracted from the sap of *Rhus succedanea*. *Journal of Natural Products*, 65(11), 1719–1721. <https://doi.org/10.1021/np0201467>
- Yang, H., Yang, M., Ding, Y., Liu, Y., Lou, Z., Zhou, Z., Sun, L., Mo, L., Ye, S., Pang, H., Gao, G. F., Anand, K., Bartlam, M., Hilgenfeld, R., & Rao, Z. (2003). The crystal structures of severe acute respiratory syndrome virus main protease and its complex with an inhibitor. *Proceedings of the National Academy of Sciences of the United States of America*, 100(23), 13190–13195. <https://doi.org/10.1073/pnas.1835675100>
- Zembower, D. E., Lin, Y. M., Flavin, M. T., Chen, F. C., & Korba, B. E. (1998). Robustaflavone, a potential non-nucleoside anti-hepatitis B agent. *Antiviral Research*, 39(2), 81–88. [https://doi.org/10.1016/S0166-3542\(98\)00033-3](https://doi.org/10.1016/S0166-3542(98)00033-3)
- Zhang, L., Lin, D., Sun, X., Curth, U., Drosten, C., Sauerhering, L., Becker, S., Rox, K., & Hilgenfeld, R. (2020). Crystal structure of SARS-CoV-2 main protease provides a basis for design of improved α -ketoamide inhibitors. *Science*, 368(6489), eabb3405–412. <https://doi.org/10.1126/science.abb3405>